Trends in Chemistry

CellPress REVIEWS

Review

Chemo-Mechanical Challenges in Solid-State Batteries

John A. Lewis,[1] Jared Tippens,[2] Francisco Javier Quintero Cortes,[1] and Matthew T. McDowell[1,2,*]

Solid-state batteries (SSBs) could exhibit improved safety and energy density compared with traditional lithium-ion systems, but fundamental challenges exist in integrating solid-state electrolytes with electrode materials. In particular, the (electro)chemical evolution of electrode materials and interfaces can often be linked to mechanical degradation due to the all-solid nature of these systems. This review presents recent progress in understanding the coupling between chemistry and mechanics in solid-state batteries, with a focus on three important phenomena: (i) lithium filament growth through solid-state electrolytes, (ii) structural and mechanical evolution at chemically unstable interfaces, and (iii) chemo-mechanical effects within solid-state composite electrodes. Building on recent progress, overcoming chemo-mechanical challenges in solid-state batteries will require new *in situ* characterization methods and efforts to control evolution of interfaces.

Highlights

Solid-state electrolytes (SSEs) can transmit stress and strain at interfaces, making solid-state batteries susceptible to chemo-mechanical degradation during electrochemical cycling.

Most Li/SSE interfaces are chemically unstable and evolve to form an interphase layer with different structure and properties.

Understanding these chemo-mechanical phenomena requires the use of advanced *in situ* and *operando* characterization techniques and correlated modeling.

The development of high-performance solid-state batteries will require control over the evolution and reactivity of interfaces.

The Intersection of Chemistry and Mechanics in Solid-State Batteries

SSBs offer the potential for improved safety and energy density compared with lithium-ion (Li-ion) batteries. These advantages arise from the use of a solid-state ion conductor instead of the flammable liquid electrolytes found in Li-ion batteries, reducing risk of fire and potentially enabling new anode chemistries [1,2]. A common SSB architecture features a lithium metal or composite particulate anode, a composite cathode, and a **solid-state electrolyte (SSE)** (see Glossary) membrane separating the electrodes (Figure 1, Key Figure). Lithium metal anodes are of particular interest for SSBs because they could enable ~50% higher energy densities than conventional Li-ion batteries [3,4].

In recent years, the development of SSBs has been accelerated by the discovery of a variety of promising SSE materials with high ionic conductivity between 10^{-4} and 10^{-2} S cm^{-1} [5–8]. A significant roadblock, however, lies in integrating SSEs with the other components of the battery. Specifically, the interfaces between SSEs and electrode materials present fundamental scientific and engineering challenges that manifest in different ways (Figure 1) [9,10]. In some SSE materials paired with lithium anodes, lithium metal has been observed to mechanically penetrate the Li/SSE interface during electrodeposition and extend through the bulk of the SSE, resulting in short circuits and cell failure (Figure 1A) [11,12]. In addition, many Li/SSE interfaces are thermodynamically unstable [13,14], with structural and chemical changes that naturally occur upon contact and electrochemical operation that can alter ion transport characteristics and mechanical integrity (Figure 1B) [15,16]. Finally, solid-state **composite electrodes** featuring densified mixtures of active material particles within an SSE matrix exhibit complex **chemo-mechanics** at interfaces, where even small strains in the active material due to ion insertion/removal can be transmitted across the interface to mechanically damage the SSE and inhibit ion transport (Figure 1C) [17–19].

The unifying feature that underlies these different phenomena is the coupling between chemical evolution and mechanical effects at solid-state interfaces. This coupling can be present whenever

[1]School of Materials Science and Engineering, Georgia Institute of Technology, 771 Ferst Drive, Atlanta, GA 30332, USA
[2]George W. Woodruff School of Mechanical Engineering, Georgia Institute of Technology, 801 Ferst Drive, Atlanta, GA 30332, USA

*Correspondence: mattmcdowell@gatech.edu (M.T. McDowell).

an (electro)chemical change, such as lithium metal electrodeposition or ion insertion, induces mechanical stress at an interface. In general, chemo-mechanical phenomena will manifest more acutely in solid-state systems compared with conventional liquid electrolyte-based batteries. This is because stress and strain can be transmitted more effectively in solid-state systems, whereas liquid electrolytes in conventional batteries cannot sustain shear stress or strain and thus act to relieve electrochemically induced strain. While it is becoming increasingly recognized that chemo-mechanical effects play an outsized role in determining the behavior and stability of SSBs [17,19,20], coupled chemical and mechanical evolution at interfaces during battery operation, and its effects on electrochemical stability, are just beginning to be understood. In many cases, *in situ* and *operando* experiments have been critical for elucidating the evolution of materials and interfaces [15,20–23], since dynamic changes at buried solid-state interfaces are difficult to probe with *ex situ* techniques. Furthermore, modeling has played an important role in predicting the chemical nature and mechanical effects at SSB interfaces [13,14,24,25]. This review presents recent progress in understanding the links between chemistry and mechanics at SSB interfaces with specific focus on the three phenomena highlighted above. We also emphasize the areas in which *in situ* characterization has been used to study chemo-mechanical phenomena, as well as future opportunities to employ these advanced techniques. Further dedicated research in this area is necessary for the creation of SSBs with improved stability and energy density for long-term operation.

Lithium Metal Filament Growth

Filamentary or dendritic growth of lithium in liquid electrolytes is a well-known challenge that can cause dangerous short circuits and has prevented the use of lithium metal anodes in rechargeable liquid-based batteries [26]. SSEs have emerged as potential options to prevent filamentary lithium growth due to predictions that the increased mechanical stiffness of SSE materials could block the growth of filaments. Assuming linear-elastic mechanical deformation behavior, Monroe and Newman showed that a polymer membrane with a shear modulus greater than twice that of lithium metal would act to block lithium filament penetration (termed 'interfacial roughening') [27]. This 'Monroe-Newman' criterion has guided the design of many SSEs, but since its development, it has been discovered that many inorganic SSEs (such as garnets and sulfides) are susceptible to lithium metal penetration and short-circuiting during electrodeposition (Figure 1A), despite being much stiffer than lithium metal [11,12,20,28–30]. The observation of lithium metal penetration in SSEs indicates a significant gap in the understanding of the links between the mechanical properties, interfacial electrochemistry, and morphological evolution of lithium metal. In particular, recent findings related to the somewhat unusual mechanical properties of lithium metal [31–37] (e.g., extensive deformation via creep) highlight the importance of understanding how mechanical properties affect interfacial electrochemical behavior and filament growth. Since a significant motivating factor for the use of SSEs is their potential compatibility with high-capacity lithium metal anodes, this short-circuiting phenomenon is a critical challenge to overcome.

Lithium metal penetration during battery cycling has been observed in multiple types of SSEs [20,38,39], but the research community has primarily focused on investigating garnet-structured $Li_7La_3Zr_2O_{12}$ (LLZO) due to its high ionic conductivity (0.1–1.0 mS cm^{-1}) and relative stability in contact with lithium metal [5,13,40]. When operating above a **critical current density (CCD)**, lithium metal filaments have been observed to grow through dense ceramic LLZO pellets despite this material's high shear modulus of ~60 GPa [11,12,41,42]. Lithium preferentially grows along grain boundaries, and internal voids can also act as growth pathways [43]. Figure 2A shows the growth pattern of lithium metal along grain boundaries in polycrystalline LLZO, revealing a web of lithium metal in the bulk material. Certain amorphous SSEs, such as lithium phosphorus oxynitride

Glossary

Chemo-mechanics: the interplay between chemistry and mechanics. In batteries, chemo-mechanics typically manifests as reactions (chemical or electrochemical) driving a mechanical response in a material, such as an electrode particle expanding during the insertion of Li. Conversely, chemo-mechanics can also involve mechanical forces driving chemical changes, such as altering the chemical potential of a system.

Composite electrode: a mixture consisting of an active electrode material and a solid-state electrolyte (typically as particles). Additives such as conductive carbon can be included to enhance transport properties within the composite.

Critical current density (CCD): the current density at which lithium metal first penetrates through a solid-state electrolyte in an electrochemical cell, causing a short-circuit. At current densities below this value, cells can be stably cycled without short-circuiting.

Interphase: a phase or mixture of phases that forms at the interface between an electrolyte material and an electrode material in a battery due to chemical or electrochemical reactions.

Mixed ionic-electronic conductor (MIEC): a phase that is both an ionic and electronic conductor. In solid-state electrolytes, the formation of MIECs within the electrolyte is detrimental due to the inability of MIECs to passivate against electrochemical reduction.

Solid-state electrolyte (SSE): a solid material with high ionic conductivity (typically greater than 10^{-4} S cm^{-1} at room temperature) and low electronic conductivity (typically less than 10^{-8} S cm^{-1}) that allows for ion transport between the anode and cathode in an electrochemical cell.

Key Figure

Chemo-Mechanical Phenomena in Solid-State Batteries (SSBs)

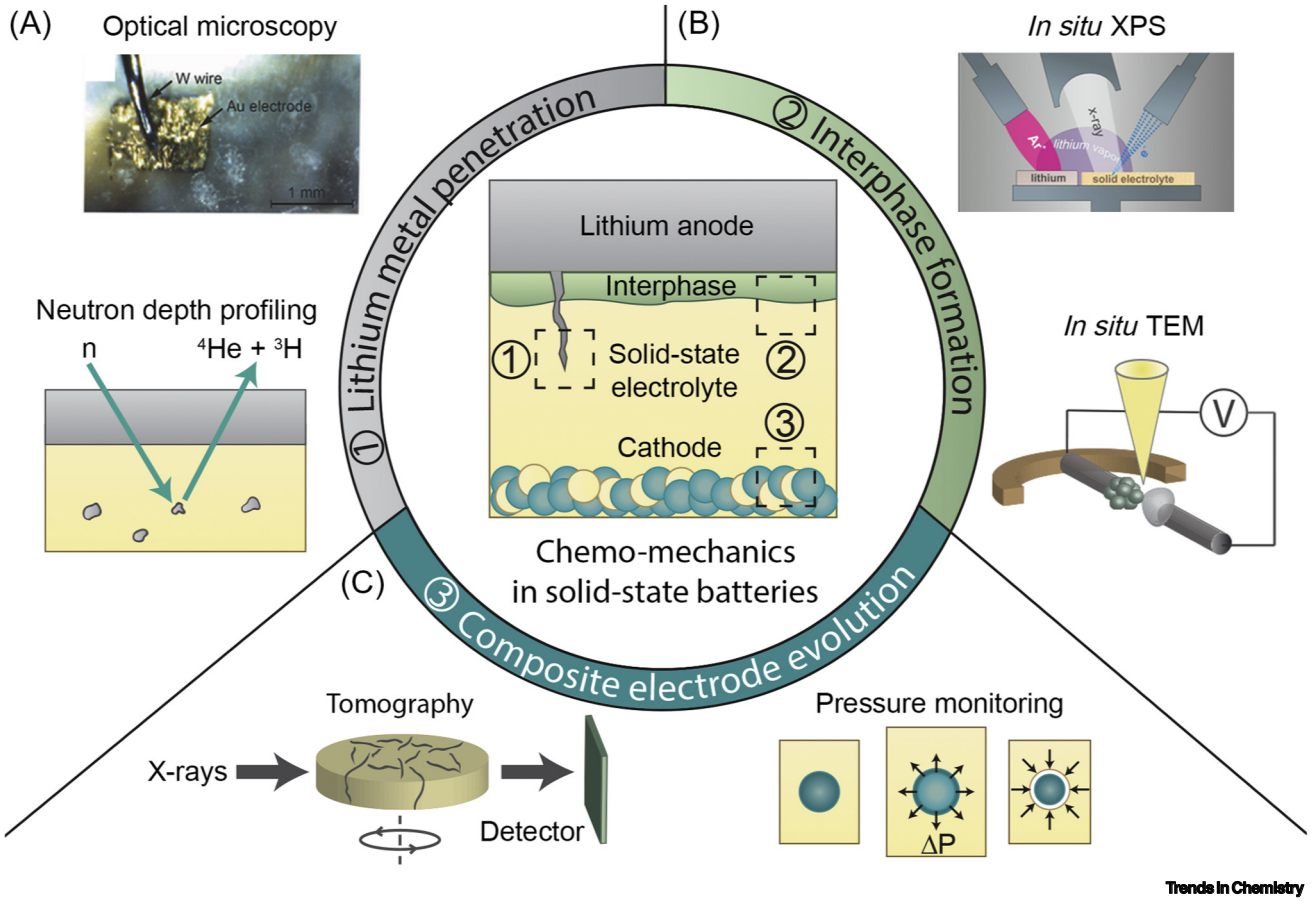

Figure 1. The center schematic shows an SSB containing a lithium metal anode, a solid-state electrolyte (SSE), and a composite cathode. At Li/SSE interfaces, electrodeposition of lithium metal can drive mechanical penetration through the SSE (labeled as 1). The SSE can also be (electro)chemically reduced to form an interphase that may have undesirable properties (labeled as 2). In composite electrodes, electrochemical reactions can create significant mechanical deformation at the SSE/electrode interface (labeled as 3). These chemo-mechanical phenomena are often difficult to characterize due to being buried within the solid, making *in situ* and *operando* characterization necessary to understand their behavior. Examples of characterization techniques that have been used to characterize chemo-mechanical behavior at SSB interfaces are shown around the ring in (A–C). The optical microscopy image in (A) is reproduced, with permission, from [20]. The *in situ* X-ray photoelectron spectroscopy (XPS) schematic in (B) is reproduced, with permission, from [75]. Abbreviations: TEM, transmission electron microscopy.

(LiPON), have been observed to form lithium filaments along interfaces (Figure 2B), but this material resists lithium metal penetration in its pure state [44]. However, single-crystalline LLZO can still experience lithium filament formation, despite the absence of grain boundaries [20]. Understanding the mechanical and chemical properties of grain boundaries and their impact on lithium metal filament suppression has been an active research area [45,46]. Studies have also postulated that the difference between the ionic conductivity of bulk and grain boundary regions in SSEs can drive lithium metal plating along grain boundaries [47–50]. In a similar vein, the bulk ionic conductivity and operating temperature have been shown to impact the observed CCD for filament growth [29,51]. Finally, other work has suggested that high interfacial impedance and nonuniform physical

contact between lithium metal and SSEs can lead to filament formation [47]. Taken together, abundant evidence has shown that the bulk elastic modulus of SSEs is not the primary factor that controls filamentary growth in many materials and that plastic deformation of lithium and local defects or perturbations must be considered.

It has become increasingly evident in recent years that the local chemo-mechanical environment during lithium metal plating and stripping at the interface with the SSE is more complex than originally thought, and this is one reason for the divergence from predictions. Using *in situ* optical microscopy (Figure 1A), Porz and colleagues showed that lithium metal filaments form at physical surface defects in several different inorganic SSE materials [20]. They proposed a mechanism in which lithium metal electrodeposition first occurs at surface flaws when operating above a CCD, which can drive crack growth within the brittle ceramic SSE. Lithium metal can then plate into the newly-opened crack, and the filling of this void space with lithium causes additional stress to build at the crack tip, which in turn further drives crack growth. According to their fracture mechanics-based model (Figure 2C), larger surface defects (such as scratches or pores) favor lithium filament growth. Eliminating initial surface flaws or modifying the local chemo-mechanical environment by engineering interfaces could thus be promising routes to preventing filament growth and short-circuiting.

In addition to *in situ* optical characterization [20,52], nondestructive acoustic characterization has also been used to track mechanical degradation in SSEs prior to short-circuiting, where the measured elastic modulus suddenly decreases at the CCD for short-circuiting [53]. *In situ/operando* neutron depth profiling experiments have also proven to be useful for detecting the presence of lithium metal filaments within SSEs (Figure 1A) [21,54]. Recent *operando* neutron depth-profiling experiments by Han and colleagues have challenged the conventional theory that filaments nucleate at the SSE/Li interface [21]. Figure 2D shows the lithium concentration measured within the bulk of an LLZO SSE during operation. As the cell is discharged (increasing time), the concentration of lithium in LLZO increases throughout the bulk region but remains constant as a function of depth (x-axis). The addition of lithium in the bulk suggests the formation of lithium metal, but the uniform concentration distribution is counter to traditional dendritic growth where a concentration gradient is present. The absence of such a gradient suggests that the electronic conductivity of SSEs may give rise to lithium metal growth directly within the bulk of the SSE [21]. If confirmed, this finding introduces another level of complexity in controlling lithium metal growth and indicates the need for SSEs with lower electronic conductivity.

To overcome the effects of filament growth, various efforts have been made to increase the CCD for short-circuiting (and thus the critical overpotential, which may be a more appropriate variable that determines short-circuiting [21]). Some studies have focused on understanding and eliminating the presence of grain boundaries in SSEs due to their observed role in filament propagation [55,56]. Other strategies have investigated incorporating a second phase into the SSE [57,58] and forming protection layers that react with lithium metal [59]. Establishing excellent 'chemical wettability' between lithium metal and the SSE has emerged as a key challenge to improve interfacial contact and reduce current nonuniformities. Enhanced wettability has been achieved by depositing various metals and oxides on the surface of the SSE [60–63]. The wettability of lithium on LLZO can also be significantly improved by removing carbonate and hydroxide surface contamination via heat treatments [64]. These strategies can effectively reduce the interfacial impedance to less than 5 Ω cm^2 and increase the CCD. Studies have also shown success in filament suppression by engineering polymer electrolytes [65], stacking layers of electrolyte materials with different properties [66–68], and using composite SSEs to reduce short-circuiting and filamentary growth [69]. These various efforts have shown promise for reducing the extent of filament

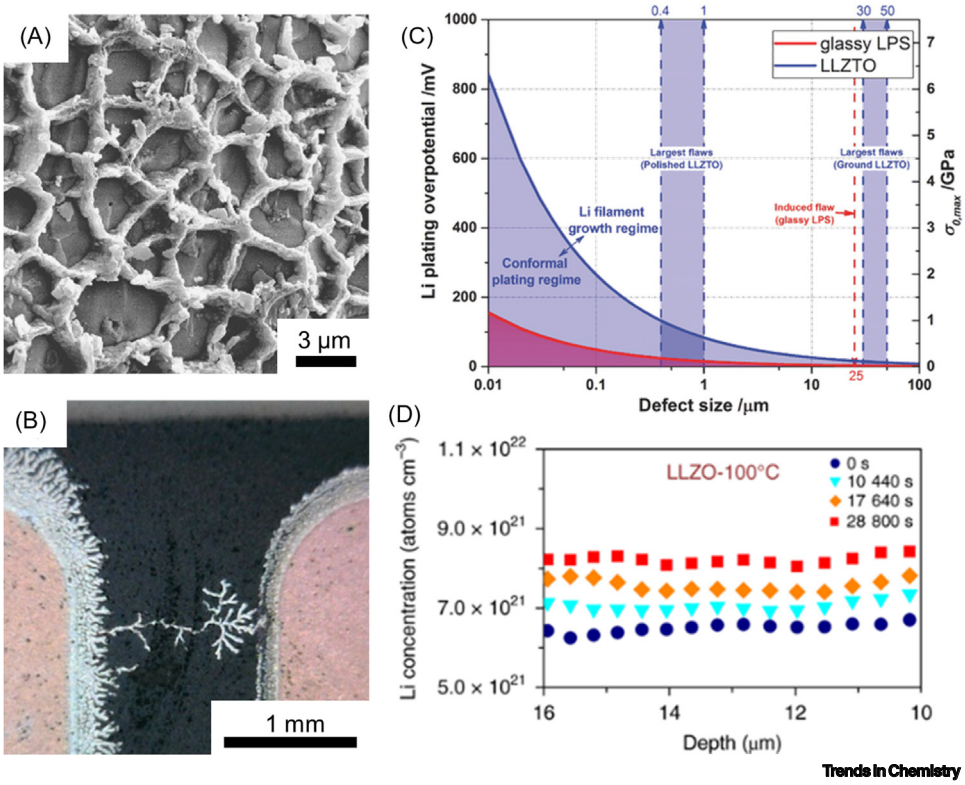

Figure 2. Lithium Metal Filament Growth. (A) Scanning electron microscopy image showing web-like lithium metal growth along grain boundaries in the bulk of $Li_7La_3Zr_2O_{12}$ (LLZO). Reproduced, with permission, from [11]. (B) Optical-microscopy image showing lithium growth along a lithium phosphorus oxynitride (LiPON) interface to connect two copper current collectors. Reproduced, with permission, from [44]. (C) A model developed by Porz and colleagues predicts that defect size at the surface of an solid-state electrolyte (SSE) is linked to the overpotential for lithium plating and thus filamentary growth of lithium through SSEs. Reproduced, with permission, from [20]. (D) Neutron depth-profiling results showing the concentration of lithium species within the bulk of an SSE during operation of a cell [21]. The increase in lithium concentration over time combined with the uniform concentration profile as a function of depth suggests that lithium metal is deposited within the bulk of the SSE, instead of propagating from the interface as a filament. Reproduced, with permission, from [21]. Abbreviations: LPS, $Li_7P_3S_{11}$.

formation, but more research is required to understand how these filament suppression strategies work and to link them to fundamental system dynamics. This is exemplified by recent work that has shown that dynamic pore formation within a lithium electrode due to lithium stripping at an LLZO interface can cause current constrictions and increased impedance [70], which may impact filament growth.

Despite numerous efforts, only moderate success has been achieved in preventing short-circuiting at the current densities necessary for realistic SSB operation. However, *in situ* and *operando* experiments have already been important for understanding fundamental mechanisms of lithium filament growth and they will likely play a critical role in determining how coupled chemical and mechanical phenomena at interfaces control metal filament growth in SSEs. This knowledge will be important to guide further development of high-energy SSBs in the coming years.

Transformations at Interfaces between Lithium and SSEs

Most Li^+-conducting SSEs are chemically unstable when in contact with lithium metal [13,14]. Chemical and structural transformations at interfaces often involve reduction and incorporation

of lithium within the SSE material, resulting in chemically induced volume expansion during the transformation to form an **interphase** region (Figure 1B) [15]. Since these volumetric changes are constrained by the interfacial contact between the interphase and the SSE, this naturally results in the evolution of stress that can cause mechanical damage (e.g., fracture or plastic deformation) near the interface. Moreover, the presence of mechanical stress can modify the thermodynamic driving force for (electro)chemical reactions, and stress/strain can also alter activation energies for diffusion, and therefore, diffusion kinetics [71–73]. Finally, morphological evolution of the lithium electrode, especially pore formation within lithium metal at the interface during lithium stripping, can cause dynamically changing interfacial contact and impedance [70]. This phenomenon is intrinsically linked to the pressure within the cell and has been identified as a critical bottleneck that limits current [70]. It is thus necessary to understand the coupled effects of chemical/morphological evolution and mechanical stress/strain at SSB interfaces.

SSE/lithium metal interfaces can be classified into three types [74]: (i) a thermodynamically stable interface where no interphase is formed, (ii) an unstable interface where a **mixed ionic-electronic conducting (MIEC)** interphase is formed, and (iii) an unstable interface where the interphase is ionically conductive but electronically insulating. Type-1 interfaces are most desirable because of their exceptional stability, but they do not exist in any known practical Li-based SSEs [13]. Type-2 interfaces are detrimental to long-term stability, as the mixed-conducting properties of the interphase facilitate continuous electrochemical reduction of the SSE, and therefore, interphase growth during cycling. Type-2 interfaces have been found in a variety of SSEs such as $Li_{10}GeP_2S_{12}$ (LGPS), $Li_{1+x}Al_xGe_{2-x}(PO_4)_3$ (LAGP), and $Li_{1+x}Al_xTi_{2-x}(PO_4)_3$ (LATP) [23,75]. Type-3 interfaces react to form an interphase with a limited thickness because electrons cannot be effectively transported to electrochemically reduce the SSE beneath the interphase. Examples of SSEs that form type-3 interfaces are LLZO, LiPON, and $Li_7P_3S_{11}$ (LPS) [76–78]. Therefore, it is the nature and properties of the mixture of phases within the interphase region that determine how it evolves during battery cycling.

First-principles modeling has been an effective tool for screening numerous material combinations and predicting whether interfaces are thermodynamically stable [13,14,79–82]. Figure 3A shows the predicted electrochemical stability windows of a variety of SSEs. Modeling can also be used to predict the thermodynamically expected reaction products that are formed upon oxidizing or reducing an SSE. Screening of reaction products at the Li/SSE interface is particularly useful for estimating the ionic and electronic conductivity of the interphase, as the transport properties dictate whether the interface will be type-2 or type-3 [79].

In situ and *operando* experimental observation of chemical and structural transformations at interfaces is necessary to determine the actual phases that form, as well as to understand how transformations are related to mechanical stress evolution. *In situ* sputtering of lithium metal inside the vacuum chamber of an X-ray photoelectron spectroscopy (XPS) instrument allows for the direct chemical reaction of the SSE without exposure to air [74]. *In situ* XPS experiments have shown that SSEs (e.g., LGPS, LAGP, and LiPON) become reduced in contact with lithium [23,75,77]. Shifts in binding energies of the elements within SSEs provide clues as to the new phases that have formed, enabling the classification of these interfaces as type-2 or type-3 [23,74,75,77,78]. Recently, an *operando* XPS technique has been reported in which lithium is electrochemically deposited at an SSE interface through the addition of surface charge using an electron flood gun to drive lithium migration [83]. These experiments simulate the electrochemical reaction that would occur during cycling instead of probing a purely chemical reaction. Figure 3B shows that this method can identify species present at the interface during charge and discharge (lithium deposition and stripping).

In situ transmission electron microscopy (TEM) is another method to probe nanoscale interfacial reactions. *In situ* TEM experiments involve either creating full SSB cells that are thin enough for imaging within the TEM [76], or directly forming interfaces within the TEM by bringing SSE materials into contact with lithium metal using a specialized sample holder (Figure 1B) [15,22]. Recently, these experiments have been used to observe phase transformations at the Li/LLZO interface (Figure 3C) [22], as well as structural changes and amorphization within individual LAGP particles upon reaction with lithium (Figure 3D) [15]. Electron energy loss spectroscopy (EELS) in conjunction with scanning TEM (STEM) can further provide information about local chemistry and identify chemical changes at the atomic scale. Figure 3C shows an example of EELS data, which revealed that pristine cubic LLZO is transformed to a stable, ~6 nm thick tetragonal LLZO interphase layer when in contact with lithium metal [22].

Despite our improved understanding of how composition and structure change at Li/SSE interfaces, efforts to link chemical and electrochemical reaction processes to mechanical degradation have been limited. Recent work has, however, explored the relationship between interphase formation and mechanical degradation in the NASICON-structured LAGP material [15,84,85]. LAGP (electro)chemically reacts with lithium to form an interphase region, which has an expanded volume (Figure 3D) and thus exerts a tensile stress on the underlying LAGP. The mixed-conducting nature of the interphase allows for continuous growth, creating sufficient stress within LAGP to cause fracture [15,84,85]. An important observation is that electrochemical cycling causes the spatial distribution of the interphase to be highly nonuniform and penetrate deep within the bulk of LAGP. The nonuniform morphology of the reacted phase creates stress concentrations that accelerate LAGP degradation and the onset of fracture [15]. By coupling *in situ* X-ray tomography with electrochemical cycling, macroscale chemo-mechanical fracture within LAGP was mapped and correlated with electrochemical behavior and interphase growth, as shown in Figure 3E [84]. This study showed that it is the fracture process which is primarily responsible for electrochemical degradation in this material, rather than interphase growth itself. The shift from filament-driven short-circuits as the primary failure mechanism (as in LLZO or LPS) to mechanical fracture driven by interphase growth demonstrates that the chemical stability of the Li/SSE interface plays a critical role in determining SSE failure mechanisms.

The creation of protection layers that prevent continuous interphase formation by blocking the transport of electrons and diffusion of Li atoms, while still allowing for Li^+ transport, is a viable path forward for controlling interphase evolution. Stable interfaces may be achieved by using a material that reacts with lithium to form an artificial interphase consisting of passivating components. Recent work has shown that certain nitride materials can react with lithium to form stable Li^+-transporting phases such as Li_3N [86,87], but experiments are necessary to confirm the formation of these thermodynamically expected products. Stabilized interfaces can also be created using a material that is stable against lithium but has inherently low electronic conductivity [59,88,89]. Polymers are often used to stabilize reactive interfaces, in part due to their ability to block electron transport [90–92]. However, materials that are both stable against lithium metal and electronically insulating are often poor ion conductors at room temperature, which may limit their performance at higher currents.

Further work is needed to develop a comprehensive chemo-mechanical understanding of unstable SSE interfaces. While it has been shown that interphase growth is linked to mechanical degradation in LAGP, understanding the dynamics of interphase formation in other SSEs and its relationship to mechanical effects is necessary. The evolution of lithium

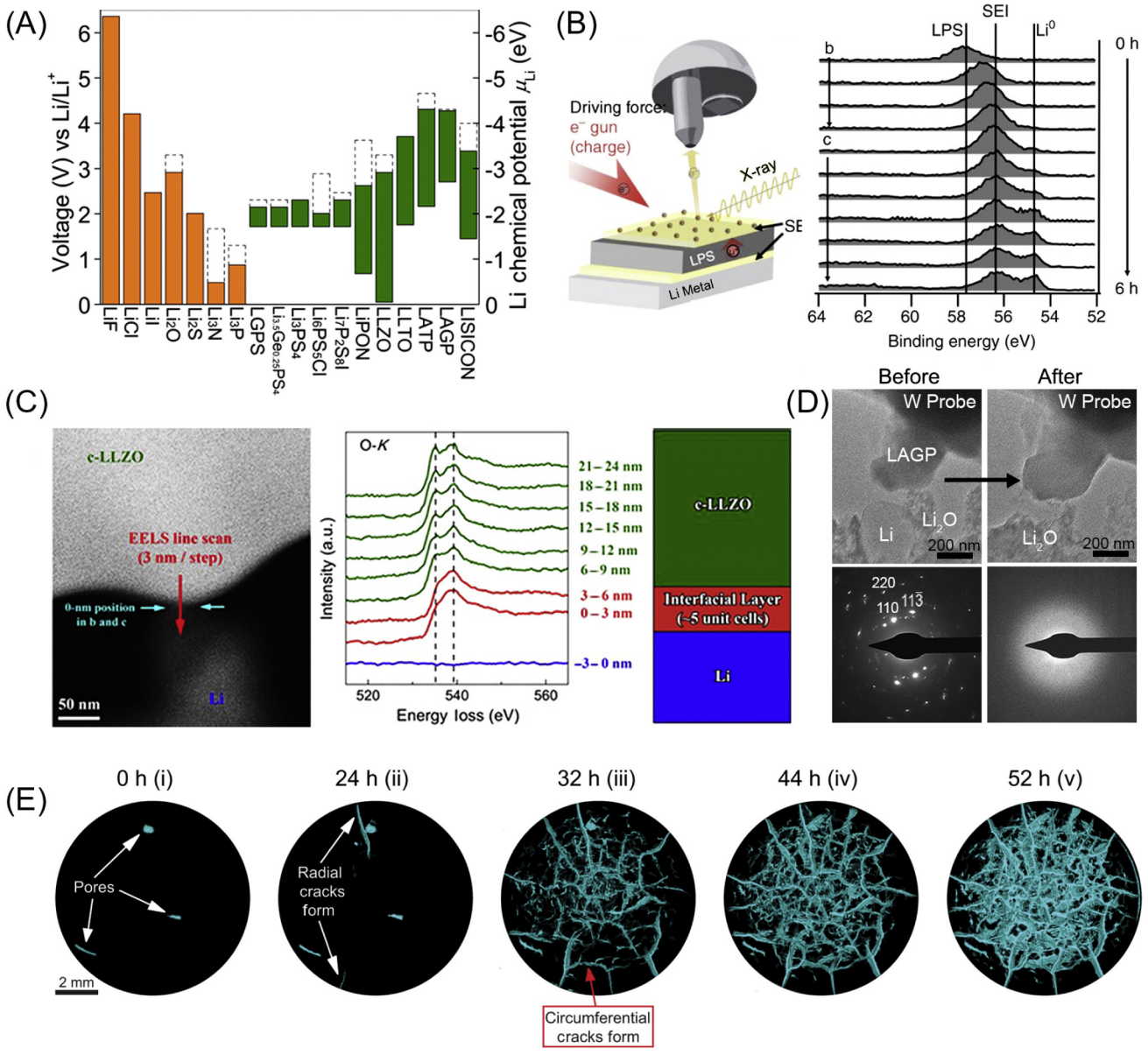

Figure 3. Transformations at Li/Solid-State Electrolyte (SSE) Interfaces. (A) Predicted electrochemical stability windows of various binary lithium compounds (orange) and common SSEs (green). Reproduced, with permission, from [13]. (B) *Operando* X-ray photoelectron spectroscopy (XPS) in which the chemical evolution of SSE interfaces with lithium is detected [83]. An electron flood gun is used to generate surface charge on the SSE, which drives Li^+ flux towards the surface (see schematic on left). This process leads to the formation of an interphase, which can be monitored in real time, as shown in the XPS spectra on the right. Reproduced, with permission, from [83]. (C) A scanning transmission electron microscopy-electron energy loss spectroscopy (STEM-EELS) line scan after *in situ* lithiation of cubic $Li_7La_3Zr_2O_{12}$ (LLZO) reveals the formation of a 6-nm thick tetragonal LLZO interphase that acts as a passivating layer and prevents further reduction. Reproduced, with permission, from [22]. (D) *In situ* transmission electron microscopy (TEM) imaging of a single $Li_{1+x}Al_xGe_{2-x}(PO_4)_3$ (LAGP) particle during lithiation shows that lithium is incorporated into LAGP, causing expansion [15]. This reaction also causes amorphization, as shown by the selected-area electron diffraction (SAED) patterns below the images. Reproduced, with permission, from [15]. (E) *In situ* X-ray tomography images of the progression of mechanical fracture within the LAGP phase in a Li/LAGP/Li cell undergoing electrochemical cycling [84]. Reproduced, with permission, from [84]. Abbreviations: LPS, Li7P3S11; SEI, solid-electrolyte interphase.

metal morphology near the interphase during deposition/stripping also requires investigation. The use of *in situ* characterization techniques (e.g., microscopy or tomography) could give insight into how different electrochemical cycling conditions influence the growth of interphases. This dynamic characterization could also be coupled with continuum mechanical modeling to understand the evolution of stress and its impact on ion transport [84]. It is also important to understand the chemistry and structure of naturally passivated (type-3) Li/SSE interfaces, as the properties of stable interphases could provide clues for creating artificial protection layers.

Interfaces within Composite Electrodes

Chemo-mechanical effects play a significant role at interfaces between active materials and the solid-ion-conducting phase within composite electrodes (Figure 1C). Cathodes and anodes other than lithium metal used in SSBs typically consist of active material particles surrounded by an SSE matrix to provide abundant ion transport pathways to the active material. As in liquid-electrolyte systems, active material particles mechanically deform during electrochemical reactions due to ion insertion and removal. The expansion and contraction of these particles can exert stress on the SSE matrix during cycling, which can cause microcracks in the SSE or delamination at the interface that isolates particles from conduction pathways [17,18,25,93]. Furthermore, these interfaces can also be electrochemically unstable, resulting in the formation of interphases with increased impedance [17,93–98]. Understanding and controlling the chemical and mechanical evolution of interfaces within composite electrodes is therefore essential to enable rechargeable SSBs with long lifetimes.

Finite-element modeling coupled with other methods (such as kinetic Monte Carlo methods to account for diffusion or cohesive-zone fracture methods to predict crack growth) can be applied to understand chemo-mechanical behavior in complex solid electrodes during electrochemical reactions [24,25,99,100]. Qualitatively, such models have demonstrated key trends that facilitate the design of solid-state composite electrodes. The size of electrode particles plays a critical role in the mechanical stability of interfaces; smaller electrode particles have higher surface area to volume ratios, which can reduce compressive stresses in the particles during lithiation (Figure 4A,B) and enhance electronic conduction pathways [100,101]. Modeling has also shown that using an elastically compliant SSE, such as a sulfide, can be both beneficial and detrimental to interfacial stability. Compliant SSEs are advantageous because they can deform more readily in response to volume changes of active particles, making them more resistant to delamination at the particle/SSE interface during particle contraction [24]. However, nonlinear kinematic modeling has predicted that compliant SSEs may be more susceptible to microcrack formation during particle expansion because they can accommodate larger deformations [25]. This modeling has also been used to predict thresholds of mechanical properties that are necessary for SSEs to resist mechanical degradation [25].

Chemical and mechanical degradation at SSE/electrode interfaces have been experimentally observed in composite electrodes. Various SSEs become oxidized when exposed to the relatively high potentials of cathode materials during charging [17,93–98], resulting in the formation of a cathode-SSE interphase with high impedance. Performance losses can thus be partially attributed to the chemical instability and impedance of these interfaces [93,94]. However, these losses can be mitigated by incorporating protection layers that reduce the interfacial resistance [102–104]. Composite electrodes are also highly susceptible to mechanical damage caused by the volume changes of active particles during electrochemical

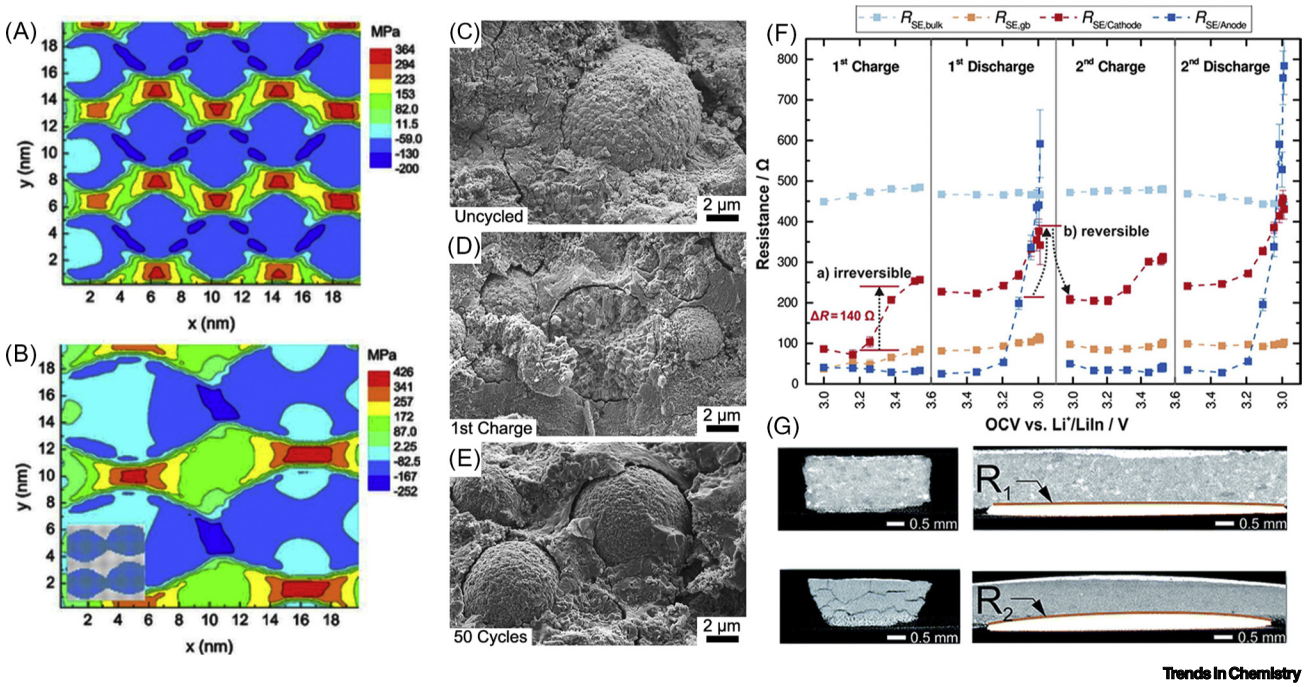

Figure 4. Chemo-Mechanics in Composite Solid-State Electrodes. (A,B) Kinetic Monte Carlo simulations combined with finite element modeling show that composites with smaller electrode particles exhibit lower mechanical stresses than those with larger particles. Reproduced, with permission, from [100]. (C) The SSE/electrode interfaces in a $LiNi_{1-x-y}Co_xMn_yO_2$ (NMC)/$Li_7P_3S_{11}$ (LPS) composite electrode initially exhibit good contact. (D) Delithiation of NMC during charging causes the electrode particles to contract and mechanically delaminate from LPS. (E) This delamination is maintained even in the discharged state where the particles have expanded. (F) In NMC/LPS composite electrodes, the SSE/cathode interfacial resistance (red markers) increases irreversibly during the first charge but exhibits reversibility in subsequent cycles, indicating the formation of an interphase during the first charge. (C–F) are reproduced, with permission, from [17]. (G) X-ray tomography of a solid-state battery before and after cycling reveals that significant bending and cracking occur as a result of electrode deformation during electrochemical reactions. Reproduced, with permission, from [18].

reactions [17,18,93]. Figure 4C–E shows that $LiNi_{1-x-y}Co_xMn_yO_2$ (NMC) particles can permanently delaminate from the SSE after the first charge due to contraction of the particles during delithiation, resulting in an increase in interfacial impedance [17]. This delamination was still present in the discharged state, despite NMC particles expanding during lithiation.

Probing chemo-mechanical phenomena at interfaces in composite electrodes using *in situ* and *operando* techniques is necessary to improve SSB performance. Electrochemical impedance spectroscopy measurements during cycling (Figure 4F) have identified that irreversible interphase formation in NMC/sulfide composite electrodes primarily occurs during the first charge and not during subsequent cycles [17]. *In situ* pressure measurements of full-cell SSBs can monitor composite electrode deformation throughout electrochemical cycling (Figure 1C) [18,19]. This method was applied to compare indium with $Li_4Ti_5O_{12}$ (LTO) anodes, which experience significantly different volume changes during electrochemical lithium insertion [18]. The negligible deformation of the LTO anode resulted in a reduction of the cell pressure throughout cycling. Maintaining smaller volume changes within a given battery system, which can result in less applied stress at SSE/electrode interfaces, may be necessary to prevent damage to the SSE. X-ray tomography has also been used to map global mechanical degradation within full SSB cells after cycling, as shown in Figure 4G [18].

Concluding Remarks

The understanding and control of solid-state interfaces has emerged as a significant scientific challenge in the development of SSB technologies. Fundamentally, the relationship between chemical/structural evolution and mechanical deformation plays a key role in the stability of such interfaces. Electrodeposition at Li/SSE interfaces can cause the growth of lithium metal filaments within the SSE, which has been linked to mechanical damage such as fracture. When the Li/SSE interface is chemically unstable, however, the formation of an interphase via (electro)chemical reduction of the SSE can also cause significant mechanical degradation. In composite electrodes, mechanical instabilities at interfaces can arise due to the inability of rigid SSEs to accommodate the electrochemically induced deformation of electrode particles during cycling.

Despite the recent progress highlighted in this review, more research is necessary in this burgeoning field to understand and control chemo-mechanical processes at SSB interfaces (see Outstanding Questions). While *in situ* and *operando* experiments have already yielded important knowledge, the application of new techniques in the future will provide critical information. For instance, tomographic imaging at different length scales, as well as spectroscopy of buried interfaces, are possible with synchrotron X-ray techniques [105], but their application to SSBs will require new experimental designs. Furthermore, the mechanical properties (e.g., modulus, strength, and plastic deformation characteristics) of newly-formed interphases, as well as their atomic and nanoscale structure, require further experimental investigation. This information is required for accurate mechanical and chemical modeling of these systems for understanding and predicting behavior.

An important additional area that requires attention is to consolidate knowledge of how individual components or materials behave within SSBs to generate broader understanding of coupled interactions within full solid-state cells. The majority of studies discussed in this review are focused on the chemo-mechanics of a particular interface or material that is present within SSBs. While such studies are critical for building an understanding of how these batteries operate, the chemo-mechanical interactions among these components within full cells is also likely of great importance. The all-solid-state nature of these systems implies that mechanical effects can act across longer distances to affect chemical processes when compared with conventional liquid-based cells. For instance, nonuniform mechanical stresses that arise due to the deposition and stripping of a lithium metal anode may be transmitted across the SSE membrane to the composite solid-state cathode, where these stresses could affect chemo-mechanical integrity and evolution of the composite electrode during cycling. Thus, designing experiments to investigate behavior of components (materials and interfaces) within full SSBs as well as in isolation is of prime importance.

In addition to these considerations, the chemo-mechanics of hybrid or composite SSE membranes is also of future interest. For high energy density, the SSE membrane thickness must approach that of conventional separators in liquid cells (~20 μm). Manufacturing thin SSE membranes may require mixtures of inorganic and organic SSEs to take advantage of both the high ionic conductivity of inorganic SSEs and the processability of polymer SSEs [106]. Thus, the chemo-mechanical stability and behavior of such composite membranes within SSB cells during cycling requires investigation. For instance, the introduction of these additional interfaces between phases could allow for mechanical delamination, current 'hot spots', or pathways for metal filament growth. Identifying and preventing failure mechanisms within various hybrid SSE membranes will be an important step towards commercialization of SSBs.

Outstanding Questions

How can we control and mitigate chemical instabilities within solid-state batteries?

How are chemical transformations at interfaces correlated with mechanical degradation?

What fundamental properties govern lithium metal filament growth through solid-state electrolytes during battery operation?

What role does the chemical stability and morphological evolution of the Li/SSE interface play in determining failure mechanisms of solid-state batteries?

Can we design solid-state composite electrodes featuring active materials that undergo electrochemical strain during ion insertion/extraction without causing mechanical degradation at active material/solid electrolyte interfaces?

What new *in situ* and *operando* experimental techniques can be used to understand structural, chemical, and morphological evolution of materials and interfaces within solid-state batteries?

Acknowledgments

Support is acknowledged from the National Science Foundation under Award No. DMR-1652471. This work was also supported by an Early Career Faculty grant from NASA's Space Technology Research Grants Program.

References

1. Aurbach, D. *et al.* (2002) A short review of failure mechanisms of lithium metal and lithiated graphite anodes in liquid electrolyte solutions. *Solid State Ionics* 148, 405–416
2. Manthiram, A. *et al.* (2017) Lithium battery chemistries enabled by solid-state electrolytes. *Nat. Rev. Mater.* 2, 16103
3. McCloskey, B.D. (2015) Attainable gravimetric and volumetric energy density of Li-S and Li ion battery cells with solid separator-protected Li metal anodes. *J. Phys. Chem. Lett.* 6, 4581–4588
4. Albertus, P. *et al.* (2018) Status and challenges in enabling the lithium metal electrode for high-energy and low-cost rechargeable batteries. *Nat. Energy* 3, 16–21
5. Murugan, R. *et al.* (2007) Fast lithium ion conduction in garnet-type $Li_7La_3Zr_2O_{12}$. *Angew. Chem.* 46, 7778–7781
6. Kamaya, N. *et al.* (2011) A lithium superionic conductor. *Nat. Mater.* 10, 682–686
7. Thokchom, J.S. and Kumar, B. (2008) Composite effect in superionically conducting lithium aluminium germanium phosphate based glass-ceramic. *J. Power Sources* 185, 480–485
8. Mizuno, F. *et al.* (2006) High lithium ion conducting glass-ceramics in the system Li_2S-P_2S_5. *Solid State Ionics* 177, 2721–2725
9. Luntz, A.C. *et al.* (2015) Interfacial challenges in solid-state Li ion batteries. *J. Phys. Chem. Lett.* 6, 4599–4604
10. Augustyn, V. *et al.* (2018) Towards an atomistic understanding of solid-state electrochemical interfaces for energy storage. *Joule* 2, 2189–2193
11. Cheng, E.J. *et al.* (2017) Intergranular Li metal propagation through polycrystalline $Li_{6.25}Al_{0.25}La_3Zr_2O_{12}$ ceramic electrolyte. *Electrochim. Acta* 223, 85–91
12. Ren, Y. *et al.* (2015) Direct observation of lithium dendrites inside garnet-type lithium-ion solid electrolyte. *Electrochem. Commun.* 57, 27–30
13. Zhu, Y. *et al.* (2015) Origin of outstanding stability in the lithium solid electrolyte materials: insights from thermodynamic analyses based on first-principles calculations. *ACS Appl. Mater. Interfaces* 7, 23685–23693
14. Richards, W.D. *et al.* (2016) Interface stability in solid-state batteries. *Chem. Mater.* 28, 266–273
15. Lewis, J.A. *et al.* (2019) Interphase morphology between a solid-state electrolyte and lithium controls cell failure. *ACS Energy Lett.* 4, 591–599
16. Chien, P.H. *et al.* (2018) Li distribution heterogeneity in solid electrolyte $Li_{10}GeP_2S_{12}$ upon electrochemical cycling probed by ^{7}Li MRI. *J. Phys. Chem. Lett.* 9, 1990–1998
17. Koerver, R. *et al.* (2017) Capacity fade in solid-state batteries: interphase formation and chemomechanical processes in nickel-rich layered oxide cathodes and lithium thiophosphate solid electrolytes. *Chem. Mater.* 29, 5574–5582
18. Zhang, W. *et al.* (2017) (Electro)chemical expansion during cycling: monitoring the pressure changes in operating solid-state lithium batteries. *J. Mater. Chem. A* 5, 9929–9936
19. Koerver, R. *et al.* (2018) Chemo-mechanical expansion of lithium electrode materials – on the route to mechanically optimized all-solid-state batteries. *Energy Environ. Sci.* 11, 2142–2158
20. Porz, L. *et al.* (2017) Mechanism of lithium metal penetration through inorganic solid electrolytes. *Adv. Energy Mater.* 7, 1701003
21. Han, F. *et al.* (2019) High electronic conductivity as the origin of lithium dendrite formation within solid electrolytes. *Nat. Energy* 4, 187–196
22. Ma, C. *et al.* (2016) Interfacial stability of Li metal-solid electrolyte elucidated via *in situ* electron microscopy. *Nano Lett.* 16, 7030–7036
23. Wenzel, S. *et al.* (2016) Direct observation of the interfacial instability of the fast ionic conductor $Li_{10}GeP_2S_{12}$ at the lithium metal anode. *Chem. Mater.* 28, 2400–2407
24. Bucci, G. *et al.* (2018) Mechanical instability of electrode-electrolyte interfaces in solid-state batteries. *Phys. Rev. Mater.* 2, 105407
25. Bucci, G. *et al.* (2017) Modeling of internal mechanical failure of all-solid-state batteries during electrochemical cycling, and implications for battery design. *J. Mater. Chem. A* 5, 19422–19430
26. Cheng, X.B. *et al.* (2017) Toward safe lithium metal anode in rechargeable batteries: a review. *Chem. Rev.* 117, 10403–10473
27. Monroe, C. and Newman, J. (2005) The impact of elastic deformation on deposition kinetics at lithium/polymer interfaces. *J. Electrochem. Soc.* 152, A396–A404
28. Ishiguro, K. *et al.* (2013) Stability of Nb-doped cubic $Li_7La_3Zr_2O_{12}$ with lithium metal. *J. Electrochem. Soc.* 160, A1690–A1693
29. Sharafi, A. *et al.* (2016) Characterizing the Li–$Li_7La_3Zr_2O_{12}$ interface stability and kinetics as a function of temperature and current density. *J. Power Sources* 302, 135–139
30. Garcia-Mendez, R. *et al.* (2017) Effect of processing conditions of $75Li_2S$-$25P_2S_5$ solid electrolyte on its DC electrochemical behavior. *Electrochim. Acta* 237, 144–151
31. Herbert, E.G. *et al.* (2018) Nanoindentation of high-purity vapor deposited lithium films: a mechanistic rationalization of the transition from diffusion to dislocation-mediated flow. *J. Mater. Res.* 33, 1361–1368
32. Narayan, S. and Anand, L. (2018) A large deformation elastic–viscoplastic model for lithium. *Extreme Mech. Lett.* 24, 21–29
33. Masias, A. *et al.* (2019) Elastic, plastic, and creep mechanical properties of lithium metal. *J. Mater. Sci.* 54, 2585–2600
34. Wood, K.N. *et al.* (2017) Lithium metal anodes: toward an improved understanding of coupled morphological, electrochemical, and mechanical behavior. *ACS Energy Lett.* 2, 664–672
35. Xu, C. *et al.* (2017) Enhanced strength and temperature dependence of mechanical properties of Li at small scales and its implications for Li metal anodes. *Proc. Natl. Acad. Sci. U. S. A.* 114, 57–61
36. Ahmad, Z. and Viswanathan, V. (2017) Stability of electrodeposition at solid-solid interfaces and implications for metal anodes. *Phys. Rev. Lett.* 119, 056003
37. LePage, W.S. *et al.* (2019) Lithium mechanics: roles of strain rate and temperature and implications for lithium metal batteries. *J. Electrochem. Soc.* 166, A89–A97
38. Nagao, M. *et al.* (2013) In situ SEM study of a lithium deposition and dissolution mechanism in a bulk-type solid-state cell with a Li_2S-P_2S_5 solid electrolyte. *Phys. Chem. Chem. Phys.* 15, 18600–18606
39. Rosso, M. *et al.* (2006) Dendrite short-circuit and fuse effect on Li/polymer/Li cells. *Electrochim. Acta* 51, 5334–5340
40. Geiger, C.A. *et al.* (2011) Crystal chemistry and stability of "$Li_7La_3Zr_2O_{12}$" garnet: a fast lithium-ion conductor. *Inorg. Chem.* 50, 1089–1097
41. Wolfenstine, J. *et al.* (2017) Mechanical behavior of Li-ion-conducting crystalline oxide-based solid electrolytes: a brief review. *Ionics* 24, 1271–1276
42. Yu, S. *et al.* (2016) Elastic properties of the solid electrolyte $Li_7La_3Zr_2O_{12}$ (LLZO). *Chem. Mater.* 28, 197–206
43. Shen, F. *et al.* (2018) Effect of pore connectivity on Li dendrite propagation within LLZO electrolytes observed with synchrotron X-ray tomography. *ACS Energy Lett.* 3, 1056–1061
44. Westover, A.S. *et al.* (2019) Deposition and confinement of Li metal along an artificial Lipon–Lipon interface. *ACS Energy Lett.* 4, 651–655
45. Wolfenstine, J. *et al.* (2013) A preliminary investigation of fracture toughness of $Li_7La_3Zr_2O_{12}$ and its comparison to other solid Li-ion conductors. *Mater. Lett.* 96, 117–120
46. Yu, S. and Siegel, D.J. (2018) Grain boundary softening: a potential mechanism for lithium metal penetration through stiff solid electrolytes. *ACS Appl. Mater. Interfaces* 10, 38151–38158

47. Tsai, C.L. *et al.* (2016) $Li_7La_3Zr_2O_{12}$ interface modification for Li dendrite prevention. *ACS Appl. Mater. Interfaces* 8, 10617–10626
48. Cheng, L. *et al.* (2015) Effect of surface microstructure on electrochemical performance of garnet solid electrolytes. *ACS Appl. Mater. Interfaces* 7, 2073–2081
49. Tenhaeff, W.E. *et al.* (2014) Resolving the grain boundary and lattice impedance of hot-pressed $Li_7La_3Zr_2O_{12}$ garnet electrolytes. *ChemElectroChem* 1, 375–378
50. Yu, S. and Siegel, D.J. (2017) Grain boundary contributions to Li-ion transport in the solid electrolyte $Li_7La_3Zr_2O_{12}$ (LLZO). *Chem. Mater.* 29, 9639–9647
51. Raj, R. and Wolfenstine, J. (2017) Current limit diagrams for dendrite formation in solid-state electrolytes for Li-ion batteries. *J. Power Sources* 343, 119–126
52. Manalastas, W. *et al.* (2019) Mechanical failure of garnet electrolytes during Li electrodeposition observed by *in-operando* microscopy. *J. Power Sources* 412, 287–293
53. Schmidt, R.D. and Sakamoto, J. (2016) *In-situ*, non-destructive acoustic characterization of solid state electrolyte cells. *J. Power Sources* 324, 126–133
54. Wang, C. *et al.* (2017) *In situ* neutron depth profiling of lithium metal-garnet interfaces for solid state batteries. *J. Am. Chem. Soc.* 139, 14257–14264
55. Sharafi, A. *et al.* (2017) Controlling and correlating the effect of grain size with the mechanical and electrochemical properties of $Li_7La_3Zr_2O_{12}$ solid-state electrolyte. *J. Mater. Chem. A* 5, 21491–21504
56. Kataoka, K. *et al.* (2018) Lithium-ion conducting oxide single crystal as solid electrolyte for advanced lithium battery application. *Sci. Rep.* 8, 9965
57. Han, F. *et al.* (2018) Suppressing Li dendrite formation in Li_2S-P_2S_5 solid electrolyte by LiI incorporation. *Adv. Energy Mater.* 8, 1703644
58. Xu, B. *et al.* (2017) Li_3PO_4-added garnet-type $Li_{6.5}La_3Zr_{1.5}Ta_{0.5}O_{12}$ for Li-dendrite suppression. *J. Power Sources* 354, 68–73
59. Xu, R. *et al.* (2018) Interface engineering of sulfide electrolytes for all-solid-state lithium batteries. *Nano Energy* 53, 958–966
60. Han, X. *et al.* (2016) Negating interfacial impedance in garnet-based solid-state Li metal batteries. *Nat. Mater.* 16, 572–579
61. Luo, W. *et al.* (2017) Reducing interfacial resistance between garnet-structured solid-state electrolyte and Li-metal anode by a germanium layer. *Adv. Mater.* 29, 1606042
62. Luo, W. *et al.* (2016) Transition from superlithiophobicity to superlithiophilicity of garnet solid-state electrolyte. *J. Am. Chem. Soc.* 138, 12258–12262
63. Wang, C. *et al.* (2017) Conformal, nanoscale ZnO surface modification of garnet-based solid-state electrolyte for lithium metal anodes. *Nano Lett.* 17, 565–571
64. Sharafi, A. *et al.* (2017) Surface chemistry mechanism of ultra-low interfacial resistance in the solid-state electrolyte $Li_7La_3Zr_2O_{12}$. *Chem. Mater.* 29, 7961–7968
65. Khurana, R. *et al.* (2014) Suppression of lithium dendrite growth using cross-linked polyethylene/poly(ethylene oxide) electrolytes: a new approach for practical lithium-metal polymer batteries. *J. Am. Chem. Soc.* 136, 7395–7402
66. Hitz, G.T. *et al.* (2019) High-rate lithium cycling in a scalable trilayer Li-garnet-electrolyte architecture. *Mater. Today* 22, 50–57
67. Duan, H. *et al.* (2018) Dendrite-free Li-metal battery enabled by a thin asymmetric solid electrolyte with engineered layers. *J. Am. Chem. Soc.* 140, 82–85
68. Wang, C. *et al.* (2017) Suppression of lithium dendrite formation by using LAGP-PEO (LiTFSI) composite solid electrolyte and lithium metal anode modified by PEO (LiTFSI) in all-solid-state lithium batteries. *ACS Appl. Mater. Interfaces* 9, 13694–13702
69. Zhou, D. *et al.* (2016) SiO_2 hollow nanosphere-based composite solid electrolyte for lithium metal batteries to suppress lithium dendrite growth and enhance cycle life. *Adv. Energy Mater.* 6, 1502214
70. Krauskopf, T. *et al.* (2019) Toward a fundamental understanding of the lithium metal anode in solid-state batteries – an electrochemo-mechanical study on the garnet-type solid electrolyte $Li_{6.25}Al_{0.25}La_3Zr_2O_{12}$. *ACS Appl. Mater. Interfaces* 11, 14463–14477
71. McDowell, M.T. *et al.* (2012) Studying the kinetics of crystalline silicon nanoparticle lithiation with *in situ* transmission electron microscopy. *Adv. Mater.* 24, 6034–6041
72. McDowell, M.T. *et al.* (2016) The mechanics of large-volume-change transformations in high-capacity battery materials. *Extreme Mech. Lett.* 9, 480–494
73. Tealdi, C. *et al.* (2016) Feeling the strain: enhancing ionic transport in olivine phosphate cathodes for Li- and Na-ion batteries through strain effects. *J. Mater. Chem. A* 4, 6998–7004
74. Wenzel, S. *et al.* (2015) Interphase formation on lithium solid electrolytes - an *in situ* approach to study interfacial reactions by photoelectron spectroscopy. *Solid State Ionics* 278, 98–105
75. Hartmann, P. *et al.* (2013) Degradation of NASICON-type materials in contact with lithium metal: formation of mixed conducting interphases (MCI) on solid electrolytes. *J. Phys. Chem. C* 117, 21064–21074
76. Wang, Z. *et al.* (2016) In situ STEM-EELS observation of nanoscale interfacial phenomena in all-solid-state batteries. *Nano Lett.* 16, 3760–3767
77. Schwöbel, A. *et al.* (2015) Interface reactions between LiPON and lithium studied by *in-situ* X-ray photoemission. *Solid State Ionics* 273, 51–54
78. Wenzel, S. *et al.* (2016) Interphase formation and degradation of charge transfer kinetics between a lithium metal anode and highly crystalline $Li_7P_3S_{11}$ solid electrolyte. *Solid State Ionics* 286, 24–33
79. Zhu, Y. *et al.* (2016) First principles study on electrochemical and chemical stability of solid electrolyte-electrode interfaces in all-solid-state Li-ion batteries. *J. Mater. Chem. A* 4, 3253–3266
80. Ong, S.P. *et al.* (2013) Phase stability, electrochemical stability and ionic conductivity of the $Li_{10\pm1}MP_2X_{12}$ (M = Ge, Si, Sn, Al or P, and X = O, S or Se) family of superionic conductors. *Energy Environ. Sci.* 6, 148–156
81. Mo, Y. *et al.* (2012) First principles study of the $Li_{10}GeP_2S_{12}$ lithium super ionic conductor material. *Chem. Mater.* 24, 15–17
82. Han, F. *et al.* (2016) Electrochemical stability of $Li_{10}GeP_2S_{12}$ and $Li_7La_3Zr_2O_{12}$ solid electrolytes. *Adv. Energy Mater.* 6, 1501590
83. Wood, K.N. *et al.* (2018) Operando X-ray photoelectron spectroscopy of solid electrolyte interphase formation and evolution in Li_2S-P_2S_5 solid-state electrolytes. *Nat. Commun.* 9, 2490
84. Tippens, J. *et al.* (2019) Visualizing chemomechanical degradation of a solid-state battery electrolyte. *ACS Energy Lett.* 4, 1475–1483
85. Chung, H. and Kang, B. (2017) Mechanical and thermal failure induced by contact between a $Li_{1.5}Al_{0.5}Ge_{1.5}(PO_4)_3$ solid electrolyte and Li metal in an all solid-state Li cell. *Chem. Mater.* 29, 8611–8619
86. Zhu, Y. *et al.* (2017) Strategies based on nitride materials chemistry to stabilize Li metal anode. *Adv. Sci.* 4, 1600517
87. Cheng, Q. *et al.* (2019) Stabilizing solid electrolyte-anode interface in Li-metal batteries by boron nitride-based nanocomposite coating. *Joule* 3, 1510–1522
88. Wang, C. *et al.* (2018) Stabilizing interface between $Li_{10}SnP_2S_{12}$ and Li metal by molecular layer deposition. *Nano Energy* 53, 168–174
89. Tian, Y. *et al.* (2019) Reactivity-guided interface design in Na metal solid-state batteries. *Joule* 3, 1037–1050
90. Zhou, W. *et al.* (2016) Plating a dendrite-free lithium anode with a polymer/ceramic/polymer sandwich electrolyte. *J. Am. Chem. Soc.* 138, 9385–9388
91. Hu, P. *et al.* (2019) Stabilizing the interface between sodium metal anode and sulfide-based solid-state electrolyte with an electron-blocking interlayer. *ACS Appl. Mater. Interfaces* 11, 9672–9678
92. Yu, Q. *et al.* (2019) Constructing effective interfaces for $Li_{1.5}Al_{0.5}Ge_{1.5}(PO_4)_3$ pellets to achieve room-temperature hybrid solid-state lithium metal batteries. *ACS Appl. Mater. Interfaces* 11, 9911–9918
93. Zhang, W. *et al.* (2017) Interfacial processes and influence of composite cathode microstructure controlling the performance

of all-solid-state lithium batteries. *ACS Appl. Mater. Interfaces* 9, 17835–17845
94. Zhang, W. *et al.* (2018) Degradation mechanisms at the $Li_{10}GeP_2S_{12}/LiCoO_2$ cathode interface in an all-solid-state lithium-ion battery. *ACS Appl. Mater. Interfaces* 10, 22226–22236
95. Hänsel, C. *et al.* (2016) Investigating the all-solid-state batteries based on lithium garnets and a high potential cathode-$LiMn_{1.5}Ni_{0.5}O_4$. *Nanoscale* 8, 18412–18420
96. Auvergniot, J. *et al.* (2017) Interface stability of argyrodite Li_6PS_5Cl toward $LiCoO_2$, $LiNi_{1/3}Co_{1/3}Mn_{1/3}O_2$, and $LiMn_2O_4$ in bulk all-solid-state batteries. *Chem. Mater.* 29, 3883–3890
97. Sakuda, A. *et al.* (2010) Interfacial observation between $LiCoO_2$ electrode and $Li_2S–P_2S_5$ solid electrolytes of all-solid-state lithium secondary batteries using transmission electron microscopy. *Chem. Mater.* 22, 949–956
98. Koerver, R. *et al.* (2017) Redox-active cathode interphases in solid-state batteries. *J. Mater. Chem. A* 5, 22750–22760
99. Xu, R. *et al.* (2018) Disintegration of meatball electrodes for $LiNi_xMn_yCo_zO_2$ cathode materials. *Exp. Mech.* 58, 549–559
100. Hao, F. and Mukherjee, P.P. (2018) Mesoscale analysis of the electrolyte-electrode interface in all-solid-state Li-ion batteries. *J. Electrochem. Soc.* 165, A1857–A1864
101. Bielefeld, A. *et al.* (2019) Microstructural modeling of composite cathodes for all-solid-state batteries. *J. Phys. Chem. C* 123, 1626–1634
102. Ohta, N. *et al.* (2007) $LiNbO_3$-coated $LiCoO_2$ as cathode material for all solid-state lithium secondary batteries. *Electrochem. Commun.* 9, 1486–1490
103. Ohta, N. *et al.* (2006) Enhancement of the high-rate capability of solid-state lithium batteries by nanoscale interfacial modification. *Adv. Mater.* 18, 2226–2229
104. Takada, K. *et al.* (2008) Interfacial modification for high-power solid-state lithium batteries. *Solid State Ionics* 179, 1333–1337
105. Pietsch, P. and Wood, V. (2017) X-ray tomography for lithium ion battery research: a practical guide. *Annu. Rev. Mater. Res.* 47, 451–479
106. Aetukuri, N.B. *et al.* (2015) Flexible ion-conducting composite membranes for lithium batteries. *Adv. Energy Mater.* 5, 1500265